EFFET DE L'INCLINAISON DE TENDONS SUR LA RÉPONSE HYDRO-AÉRODYNAMIQUE D'UNE ÉOLIENNE À PLATE-FORME SUR LIGNES TENDUES DE 10 MW

THE EFFECT OF TENDON INCLINATION ON THE HYDRO-AERODYNAMIC RESPONSE OF A 10 MW TENSION-LEG PLATFORM WIND TURBINE

D. MILANO[1,2,4], C. PEYRARD[1,2], M. CAPALDO[3]

daniel-externe.milano@edf.fr ; christophe.peyrard@edf.fr ; matteo.capaldo@edf.fr

[1]EDF Lab Chatou - 6 quai Watier, 78400 Chatou, France
[2]Saint-Venant Hydraulics Laboratory, 6 quai Watier, 78400 Chatou, France
[3]EDF Lab Paris - Saclay - 7 Boulevard Gaspard Monge, 91120 Palaiseau, France
[4]IDCORE - Industrial Doctoral Centre for Offshore Renewable Energy

Résumé

L'énergie éolienne flottante représente une solution prometteuse pour l'exploitation des ressources éoliennes en mer à des profondeurs moyennes à grandes. Cependant, la complexité de ces systèmes nécessite une compréhension approfondie des interactions entre la structure et les efforts incidents du vent et des vagues. Alors que de nombreuses solutions sont explorées, le secteur n'a pas encore convergé vers une conception optimale des flotteurs. Le but de cette étude est d'étudier les conséquences d'un changement de conception du système d'amarrage des éoliennes à plate-forme sur lignes tendues, en observant l'impact de l'inclinaison des tendons sur la réponse dynamique aux vagues irréguliers et au vent. Les résultats indiquent que l'optimisation de la géométrie d'amarrage peut réduire considérablement les mouvements du flotteur et les tensions dynamiques des lignes en raison de l'excitation des vagues, et minimiser l'amortissement aérodynamique négatif.

Summary

Floating wind energy represents a promising solution for harvesting offshore wind resources in medium to deep water. However, the complexity of these systems requires a deep understanding of the interactions between the structure and the incident forces from wind and waves. As numerous solutions are being explored, the industry is yet to converge towards an optimal floater design. The aim of this study is to investigate the consequences of changing the design of the mooring system of tension-leg platform (TLP) wind turbines, observing the impact of tendon inclination on the dynamic response to irregular waves and wind. The results shown in this paper indicate that mooring geometry optimisation can significantly reduce the floater's motions and line dynamic tensions due to wave excitation, as well as minimise the aerodynamic negative damping effect.

I – Introduction

The wind energy industry, in recent years, has developed technologically and grown rapidly. Higher wind energy availability offshore has encouraged significant investments in offshore wind installations. However, in waters over 50 m deep, fixed foundations are technically and economically challenging [3]. The new generation of floating offshore wind turbines (FOWTs) represents an opportunity to harvest high-energy density wind resources in intermediate and deep-water areas, which are unreachable using conventional fixed bottom designs. New solutions are being continuously explored as the industry strives to exploit high-energy wind resources at deep-water sites while reducing costs and environmental impact.

Amongst the variety of potential FOWT solutions, tension-leg platform (TLP) wind turbines are attractive due to reduced floater motions and structural forces [14]. TLP designs are characterised by exceeding buoyancy forces, where the floater is kept in place by pre-tensioned vertical or inclined mooring lines (commonly referred to as tendons) which are also responsible for the stability of the FOWT system. EDF Energies Nouvelles has recently been selected for building a pilot floating wind farm for the Provence Grande Large (PGL) project in the northern part of the Golf of Lion, about 15 km off the coast of Marseille. The project, financed by the Agence de l'environnement et de la maitrise de l'energie (ADEME), aims to install three 8MW Siemens wind turbine demonstrators on SBM TLP foundations by 2020.
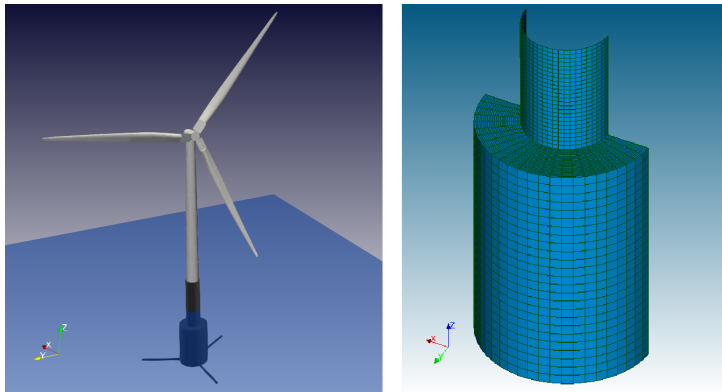

Figure 1: TLP concept of the DTU 10-MW FOWT (left) and floater mesh (right)

The study of these complex hydro-aero-servo-elastic systems requires a deep interdisciplinary understanding of the interactions between the floater hydrodynamics, turbine elasto-aerodynamics and mooring system dynamics. A good understanding of the correlation between geometric configuration and dynamic behaviour is key for the development of future TLP designs. The study presented in this paper aims to identify the effect of tendon inclination on the static and dynamic response of the DTU 10-MW Reference Wind Turbine (DTU 10MW RWT, Figure 1 - left), developed by the Technical University of Denmark (DTU) as part of the INWIND.EU project [4] [5]. Fully coupled computer-aided engineering (CAE) tools allow us to simulate FOWT's behaviour, in terms of dynamic response and power generation in the time domain, at an acceptable computational cost. The paper focusses on the impact of mooring line inclination on the FOWT behaviour when subject to different wind and wave conditions, and possible mitigation effects on aerodynamic negative damping phenomena. The fully coupled hydro-aero elastic CAE tool DIEGO/CALHYPSO, in-house developed by EDF R&D, was used for the analysis.

The fully coupled numerical tools used for FOWT modelling and running time-domain simulations are presented in the methodology section, including the main theories and assumptions considered in the analyses. The FOWT validation and prototype models are described in Sections III – 1 and III – 2, where the results of validation tests and the newly introduced design configurations are presented. The following section presents the results of the irregular wave and negative damping simulations before moving to the discussion of the findings and the conclusion of the paper.

II – Methodology

While frequency domain analyses can provide valuable insight during the design of off-shore structures, complex wave and wind interactions often require fully coupled, non-linear time domain analyses of FOWT systems. A mesh of the floater's wetted surface area was created using the CAD/CAE platform SALOME-MECA (Figure 1, right), developed by EDF R&D and CEA, and used to solve the first-order potential hydrodynamic problem on the Boundary Element Methods (BEM) code NEMOH, developed by École Centrale de Nantes, to compute the wave loads, added mass and damping coefficients [2] [8]. The resulting hydrodynamic database is used as an input for the hydrodynamic solver CALHYPSO to compute the diffraction and radiation forces on the FOWT system.

II – 1 Fully-coupled, time-domain simulations

Structural dynamics: The flexible mechanical model is described by multibody system (MBS) theory, connecting rigid and flexible bodies via kinematic constraints and force elements. The turbine rotor dynamic problem is solved using a floating frame attached to the rotor and the classic finite elements tools [1] with the addition of projection phases to include external loads defined in the inertial frame. DIEGO characterises flexible blades and tower via a linear 6DOF representation assuming small deflections within each member.

Aerodynamics: DIEGO computes local aerodynamic forces on the wind turbine blades using blade element momentum theory (BEMT) [6]. A number of empirical corrections were used, including Prandtl's formulation to consider hub and tip losses, and Glauert's correction for BEMT errors in the turbulent wake state. Dynamic stall, which stems from variations of wind velocity over the rotor disk (due to wind shear, vertical wind and yaw misalignment), is accounted for via Beddoes-Leishman formulation. Figure 2 shows the aerodynamic power and thrust curves comparison between our numerical model and DTU's results obtained using NREL's code FAST.
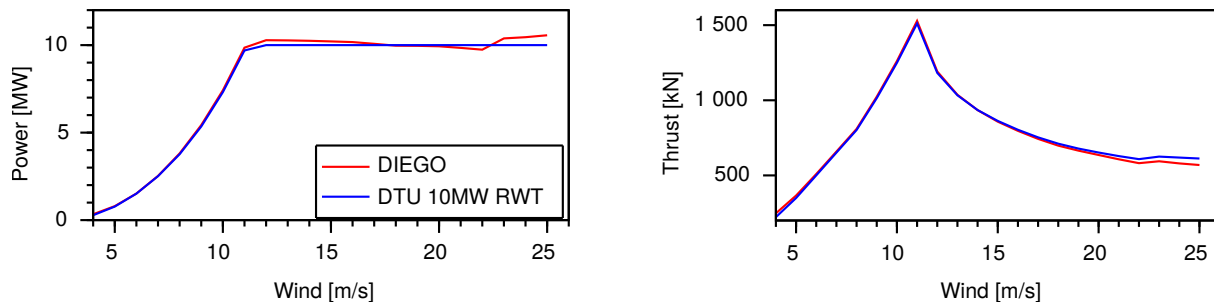

Figure 2: Aerodynamic power and thrust curves of the DTU 10-MW RWT

Control: The basic DTU Wind Energy controller was coupled with DIEGO. It was developed for pitch-regulated, variable speed wind turbines, and features both partial and full load operation capabilities [10].

Hydrodynamics: The hydrodynamic problem is linearized, and Airy theory is used to describe the wave kinematics by neglecting higher order hydrodynamic phenomena although higher order Stokes waves can be used nonetheless [15]. Wave excitation loads are calculated using the Cummins equation [7] [9] to account for the diffraction and radiation effects, as forces, added mass and damping coefficients are previously obtained by solving the potential flow problem using NEMOH. Drag forces are taken into account via Morrison's equation, the use of which is justified by the slender geometry of the transition piece (TP).

Mooring system: Restraining forces, necessary for station-keeping against external forces, are calculated using the dynamic approach, which allows the inclusion of inertia, resonance and damping effects. The forces are calculated via finite element method (FEM), taking in consideration the elasticity of the mooring lines. As TLP systems are characterised by small floater motions and relative tendon tension variations, a linearized model is expected to provide a good approximation of the restoring behaviour of the TLP mooring system.

II – 2   Post processing

Exceedance probability: The dynamic response of the model to an irregular sea state was investigated to observe how the response changed as the inclination of the tendons was increased. Empirical exceedance probability plots present the results clearly and concisely, and are defined as:

$$P = p(X \leq x_i) = 1 - \frac{i-1}{N} \tag{1}$$

Where x_i is the i-th peak response sorted in increasing order and N is the total number of peaks. The extreme events in the dynamic response are magnified and visualised by plotting the exceedance probability on a logarithmic scale.

III – DTU 10MW FOWT Numerical model

The development of the three-bladed, upwind wind turbine is described by [4], and the design was based on the IEC class 1A wind climate. It was inspired by the NREL 5MW [12] and scaled up in order to be representative of what is believed will be the future generation of offshore wind turbines. In order to reduce the rotor's weight, FFA-W3 airfoils were chosen as they meet the requirements of high relative thickness and stiffness. The tension-leg platform concept was developed by [14] via numerical and experimental modelling, and was purposely designed for the DTU 10MW RWT. The platform is composed of two main cylindrical elements, a transition piece installed on top of a coaxial floater, and the tendons attached to three slender spokes on the bottom of the floater (Figure 1, left). All simulations were performed in a water depth of $180m$. Two versions of the turbine are used in this paper and are presented in this section.

Validation model: Based on the 1:60 basin model used and described by [14], which differs from DTU's prototype due to practical limitations of the physical model. The static and dynamic motion and line tension responses of the validation model were compared to the experimental basin test results.

Prototype: Based on the original model designed by DTU, the prototype was used for the study of tendon geometry effects. The process undertaken to choose the five tendon configurations used for the study is also explained here.

III – 1   Validation model

This study focusses on the three-legged design defined as *Structure 3* in [14], and the main properties of the validation model are presented in Table 1.

Global system		Steel pipe tendons	
Total mass	$3791.6mT$	Young's modulus	$21 \times 10^{10} Pa$
Vertical CoG	$22.68m$	Cross section area	$1.55 \times 10^{-2} m^2$
I_{xx} and I_{yy}	$1.73 \times 10^{10} kgm^2$	Stiffness EA_t	$3.25 \times 10^3 MN$

Table 1: Properties of the DTU 10MW FOWT validation model

Static equilibrium: When the FOWT is subject to a constant wind, the generated thrust load imposes a new static equilibrium on the system, measured in its centre of gravity. Steady wind velocities ranging from 4 to 25 m/s were applied to the FOWT, and the resulting static displacements in surge, heave and pitch were compared with the numerical and upscaled experimental data obtained by [14]. A simple static model including the same three degrees of freedom was also used to determine and validate the response of the rigid body model.
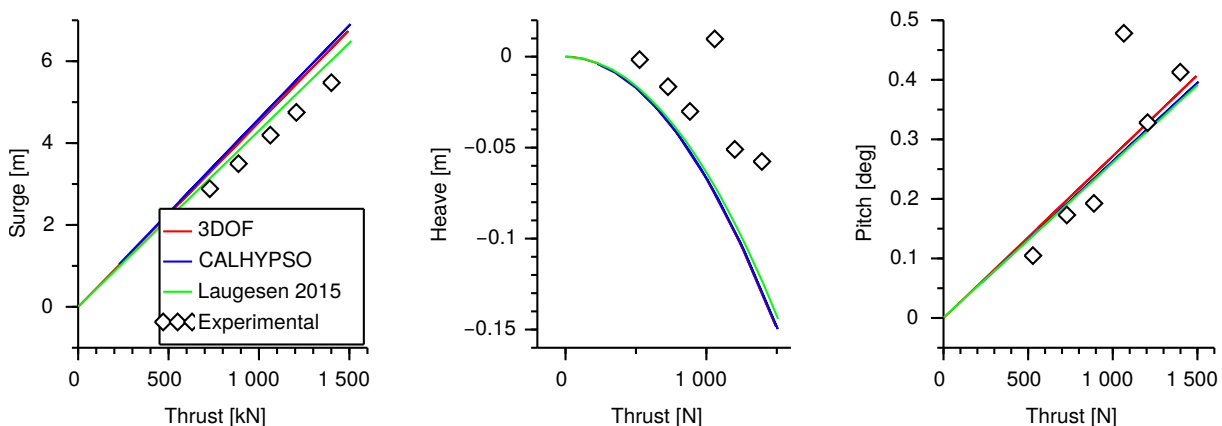

Figure 3: Static displacement of the validation model against rotor thrust

The 3DOF model includes the TLP structure, turbine and flexible mooring lines, and provides the system's 2D static displacements by balancing gravity, mooring, buoyancy and thrust forces and moments.

$$f_g + \sum_{i=1}^{3} \tau_i + f_b + f_T = 0 \tag{2}$$

and

$$r_m c, FWT \times f_g + \sum_{i=1}^{3} r_{\tau_i} \times \tau_i + r_b \times f_b + r_R NA \times f_T = 0 \tag{3}$$

Decay test: A decay test was also performed to compare the structure's natural frequencies with the experimental data. Initial displacements were globally imposed on the structure. Once released, the turbine would move back to its equilibrium position oscillating at the natural period of the observed mode. The same test was repeated for each degree of freedom of the rigid body in order to obtain the natural periods of the free structure using the Fast Fourier Transform (FFT), and the results are shown in Table 2.

DOF	Basin test [s]	CALHYPSO [s]	DOF	Basin test [s]	CALHYPSO [s]
Surge	38.7	40.0	Roll	4.3	4.7
Sway	38.7	40.0	Pitch	4.3	4.1
Heave	1.8	1.8	Yaw	11.1	11.5

Table 2: Validation model rigid body natural periods

Irregular sea state: The behaviour of the validation model was observed in a 3-hour realisation of an irregular wave climate of $H_s = 10.74m$ and $T_p = 12.4s$. The second order terms of the incident flow potential were taken into consideration via Rainey's equation [15], and the results were compared with the model's motion response to simple linear wave loads. As shown in Figure 4, however, the comparison with experimental results indicates that surge response is significantly overestimated using Rainey's formulation. The reason for this could be attributed to the fact that Rainey's equations are an extension of Morrison's equations, while the more complex quadratic transfer functions (QTF) should be used with NEMOH's hydrodynamic database. The linear wave loads were therefore used for the rest of the study (as reported in Section IV – 1), as they provide the best fit with the experimental data. The discrepancies in the heave and pitch responses were deemed acceptable due to the small motions involved and the uncertainties concerning the basin model setup and measurements, although further investigations will be necessary to better understand the interactions between the structure and irregular sea climates.
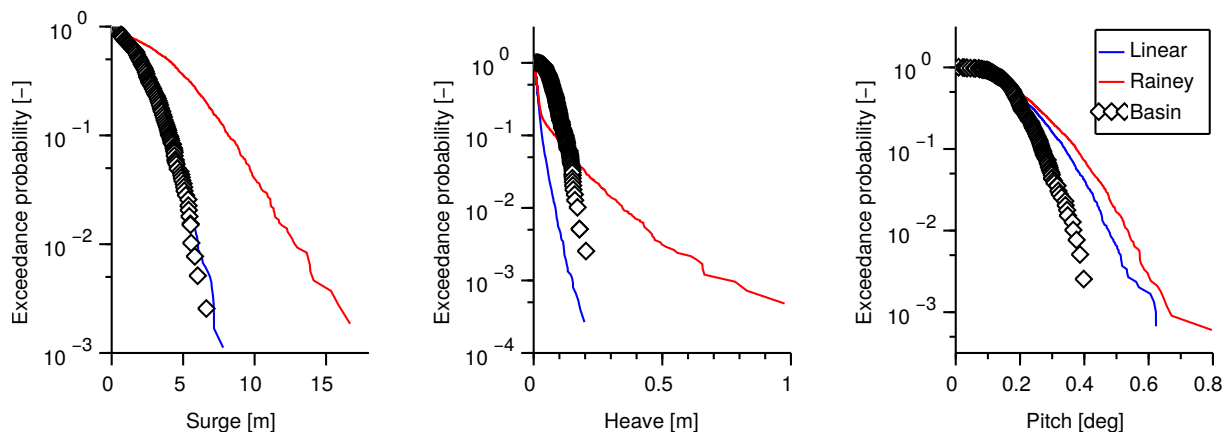

Figure 4: Motion response of the validation model to irregular sea climate

III – 2   Prototype

[14] proposes steel pipe tendons due to their frequent use in the oil and gas industry and the advantages of using neutrally buoyant tendons, as per [3]. Steel pipes are used in the oil and gas industry due to their high stiffness, as the offshore facilities are continuously

manned and require as little motion as possible. FOWTs, on the other hand, can accommodate higher platform motions and therefore softer tendons can be used. The effect of tendon inclination on the system was hence investigated using steel wire ropes instead of steel pipes. As steel wire ropes have a lower axial stiffness, higher heave and pitch motions are expected in comparison to the validation model. Bending stiffness, on the other hand, is negligible, which causes very small surge response changes between wire ropes and pipes. The main properties of the prototype model are shown in Table 3.

DTU 10MW RWT		Floater	
Rated power	$10MW$	Floater diameter	$18m$
Cut in/out wind speed	$4-25m/s$	TP diameter	$9m$
Rated wind speed	$11.4m/s$	Floater height	$25m$
Rotor speed	$6-9.6rpm$	TP height	$32m$
Maximum tip speed	$90m/s$	Spoke length	$32.1m$
Rotor diameter	$178.3m$	Submergence	$12m$
Blade length	$86.5m$	Mass	$2390mT$
Rotor height	$119m$	**Steel wire rope tendons**	
Gearbox ratio	50	Length	$142m$
RNA mass	$552mT$	Steel density	$6500kg/m^2$
Blade mass	$41.7mT$	Young's modulus	$10.69 \times 10^{10} Pa$
Tower mass	$469mT$	Cross section area	$0.093m^2$
Global system			
Vertical CoG from msl	$18.2m$	I_{xx} and I_{yy}	$1.3 \times 10^{10} kgm^2$
Displacement	$7264m^3$	I_{zz}	$8 \times 10^8 kgm^2$

Table 3: Properties of the DTU 10MW FOWT prototype model

Once the model has been validated, the sensitivity of the FOWT's motion response to tendon inclination was investigated by varying the tendon configuration. Figure 5 shows the variation in static displacement - generated by a constant 11 m/s wind along the rotor's axis at nacelle height - due to the inclination angle of the tendons, where 90deg represents the vertical configuration. The turbine model was simplified into a 6 DOF rigid body with a porous disc representing the rotor. This allowed the effect of the rotor's torque on the turbine's motion to be neglected, and for the static displacement to result purely from the thrust force in the direction of the rotor's axis.
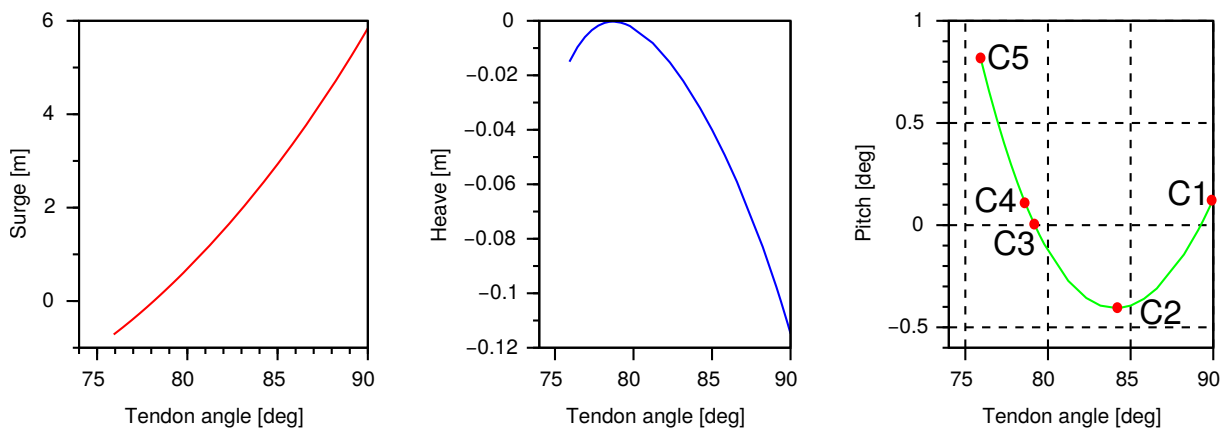

Figure 5: Static equilibrium at different tendon inclinations under steady wind of 11m/s

As shown in Figure 5 (right), the FOWT does not pitch at tendon angles 79.18deg and 89.24deg when subject to a thrust force in the nacelle. Pitch rotation (RY) is positive when the turbine is "pitching", as the turbine leans away from the wind or, in other words, the rotor moves in the direction of the wind. Pitch rotation is negative, on the other hand, when the turbine is "counter-pitching", as the turbine leans towards the wind. The zero-crossing locations in Figure 5 (right) thus represent demarcation configurations between positive RY (pitching) and negative RY (counter-pitching) behaviour. From this investigation, five configurations were chosen for the study of the impact of tendon inclination on the FOWT's dynamic response and are listed in Table 4. For clarity, the configurations are identified by the converging point of the tendons on the vertical axis.

Configuration	Convergence [m]	Inclination [deg]	Description
C1	-	90	Vertical tendons
C2	280	84.23	Maximum counter-pitch
C3	130	79.18	No pitch
C4	119	78.44	Converge at nacelle height
C5	90	75.92	Maximum pitch

Table 4: DTU 10MW FOWT Tendon configurations

IV – Results

The results of the time domain simulations are presented hereinafter. The changes of the dynamic responses to hydrodynamic and aerodynamic effects were investigated separately, in order to better understand the interaction between different excitation forces and FOWT designs. All the motions were measured in the CoG of the FOWT.

IV – 1   Irregular waves

Each tendon configuration was subject to a 3-hour realisation of an irregular wave climate of $H_s = 10.74m$ and $T_p = 12.4s$ using the JONSWAP spectrum at peak enhancment factor $\gamma = 0.9$, corresponding to *sea state 8* in [14]. As there was no wind included in the simulations for this analysis, the turbine was modelled as a rigid body and the rotor was represented by a lump mass at the top of the tower. Focus is given to the motions of the FOWT's centre of mass and the changes in the tension of the upstream tendon T1 and downstream tendons T2 and T3.

Figure 6 (top) shows the motion responses to irregular waves. The vertical tendon configuration, C1, presents the largest surge motion with peaks of $8m$ at exceedance probability $P \approx 10^{-3}$. As the tendon inclination angles increase, the surge response is significantly reduced as C5 presents peaks of less than $6m$. Heave and pitch motions, on the other hand, become wider as the tendons are inclined. From C1 to C5, heave and pitch peak responses range from $0.21m$ to $0.68m$ and from $0.2deg$ to $5deg$ respectively.

Figure 6 (bottom) shows the normalised tendon tension variations as the ratio between the i-th peak tendon tension τ_i and the initial tension at rest position τ_0. Configuration C1 presents the highest tendon responses as the upstream tendon T1 has a τ/τ_0 range of $\pm 50\%$, while downstream tendons T2 and T3 oscillate within $\pm 35\%$. The smallest tension range is given by configurations C3 and C4, as τ/τ_0 remains within a range of $\pm 22\%$ in T1 and $\pm 15\%$ in T2 and T3, hence presenting the best overall tension dynamic response to irregular sea climates.
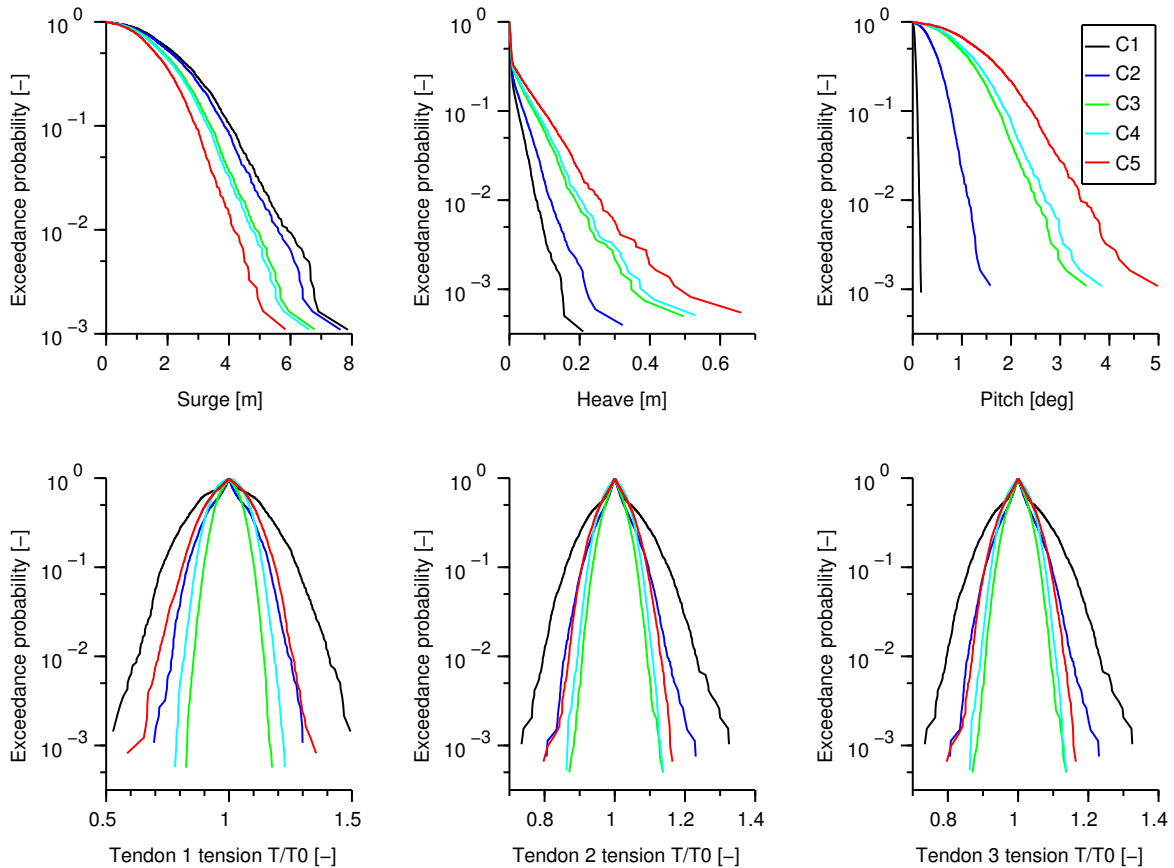
Figure 6: DTU 10MW FOWT motion and tendon tension responses to irregular sea

It is also worth noting that, between $P = 10^0$ and 7×10^{-1}, configurations C3, C4 and C5 present larger τ/τ_0 peaks than C1 and C2. This indicates that while inclined tendon configurations have a significantly better tension response to large waves (P between 7×10^{-1} and 10^{-3}), their response to small incident waves is worse than C1 and C2.

IV – 2   Negative damping

FOWTs, in comparison to bottom-fixed systems, are characterised by soft foundation properties. This causes the 6DOF natural frequencies to be significantly lower than fixed foundation structures, which can lead to resonant coupling between the turbine and the pitch controller. As the turbine moves in combination with the pitching blades, negative damping effects can induce large resonant motions in the FOWT. This can be mitigated by changing the control gains so that the pitch regulation natural period becomes higher than the highest FOWT natural period [11] [13]. The aim of this study is, however, to investigate the mitigating effect of tendon inclination without modifying the controller's parameters. As the negative damping effect takes place due to specific interactions between the FOWT and the controller, significant complexity was added to the model for the final investigation presented in this paper; aerodynamic forces on the blades are computed using BEMT, while blade and tower deformations were also included in the analysis.

A steady 15m/s wind was applied on the rotor for $2000s$, and a linear ramp of $600s$ was used to gradually bring the rotor to rated speed. Once the wind reaches the rated speed of $11.4m/s$, the controller switches from partial to full load operation. As the controller

starts adjusting the blade pitch angle to the incident wind speed ($t = 460s$) the floater starts moving in response to the oscillating aerodynamic thrust force. Figure 7 shows the motion dynamic response to steady wind of the different FOWT configurations. It is immediately noticeable that the negative damping effect has a great impact on the surge and heave motion of C1, as the oscillations amplitude is very high even once a steady state is reached between the aerodynamic (negative) and hydrodynamic (positive) damping forces.

The range of surge oscillation is reduced from $7m$ to $1.1m$ when moving from C1 to C2, and is basically zeroed at C3, C4 and C5. Heave responses have the same trends, although at a lower order of magnitude. The pitch response to the variable blade angle of attack is significant at C2 and C5, representing respectively the configurations with the maximum pitching and maximum counter-pitching behaviour. It is clear, however, that hydrodynamic damping has a lower impact on the counter-pitching design C2, as the oscillation amplitude remains higher over time, while it reduces significantly in C5. Configuration C4 presents the most favourable dynamic response.
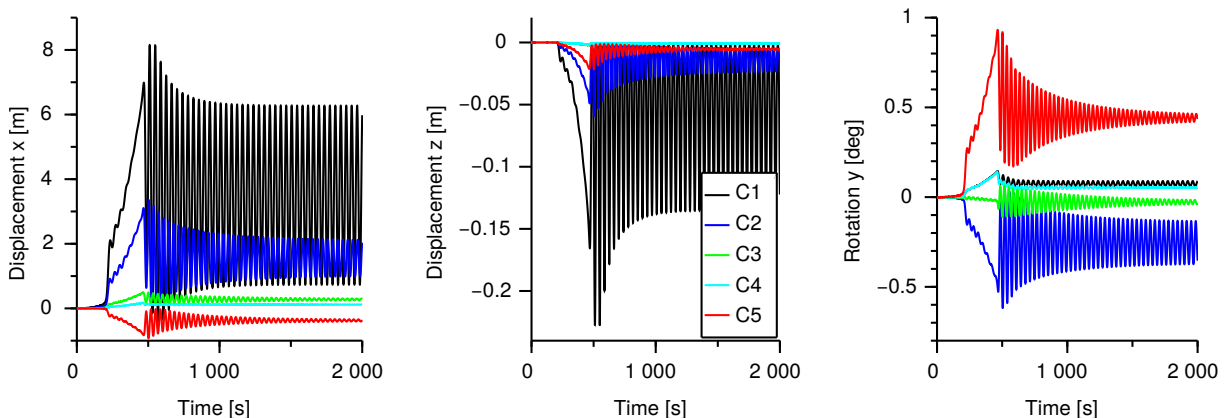

Figure 7: Negative damping on DTU 10MW FOWT motions at 15 m/s wind speed

V – Discussion

The results presented in the previous section are discussed in detail here, with the aim of identifying the underlying physics of the observed hydrodynamic effects and structural responses.

V – 1   Pitching and counter-pitching designs

The pitching behaviour of the turbine is a key aspect of a FOWT design. As shown in Figure 5, tendon inclination affects the way the floating turbine moves in reaction to rotor aerodynamic thrust. Whether the turbine will pitch or counter-pitch depends on the position of the system's centre of rotation (CoR) on the vertical z axis. The CoR is the fixed point around which a moving body rotates. If the CoR is somewhere on the moving body, the body is undergoing pure rotation, while if the CoR is outside, the body is undergoing a combined rotation and translation along a circular arc.

Given two points A and B on a moving body, as per Figure 8 (left), let Δr_a and Δr_b be segments connecting the points at the instant t to the same points at the instant t' - A' and B'. The centre of rotation O is identified as the intersection of the perpendicular
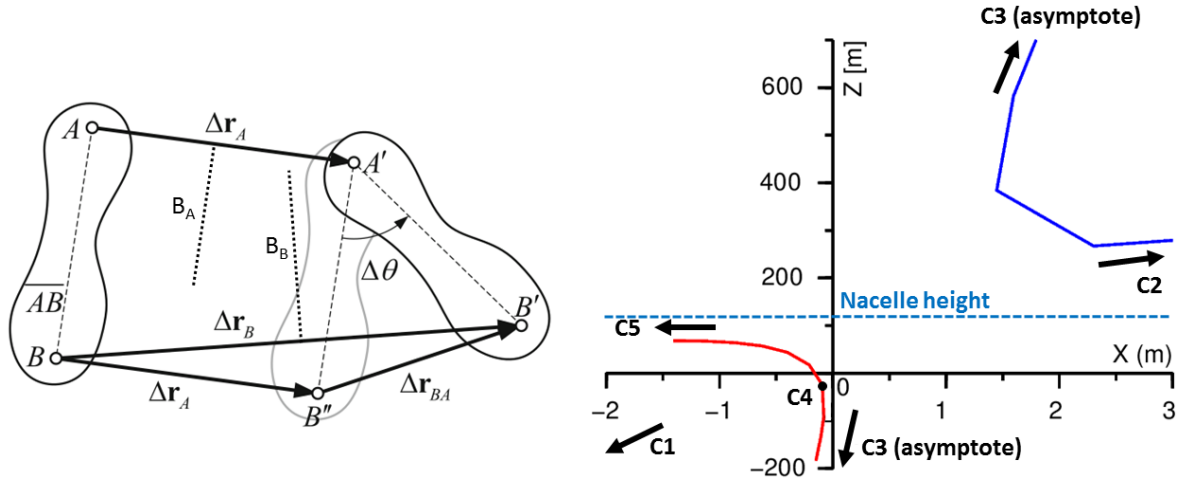
Figure 8: Rotation of a rigid body (left) and CoR in the DTU 10MW FOWT (right)

bisectors B_A and B_B of the segments. Based on this method, Figure 8 (right), shows the change in the CoR position in function of the tendons inclination. The FOWT will therefore pitch when the CoR is below the nacelle, and counter-pitch when the CoR is above it. As C3 does not have a CoR, the graph approaches it asymptotically.

V − 2   Tendon tension response in frequency domain

Configurations C3 and C4 showed the best performance in terms of tension response in all three tendons when subject to large waves. However, the opposite was observed with the smallest waves in the spectrum, as the response amplitude in C3, C4 and C5 close to $P = 10^0$ was higher than the one observed in C1 and C2. This can be explained by the higher tension frequency response of C3, C4 and C5 in the $0.3 − 0.4Hz$ range, which is the natural frequency range of pitch and roll. Figure 9 shows the FFT of the irregular sea surface elevation, pitch motion and normalised tension of the upstream tendon T1.
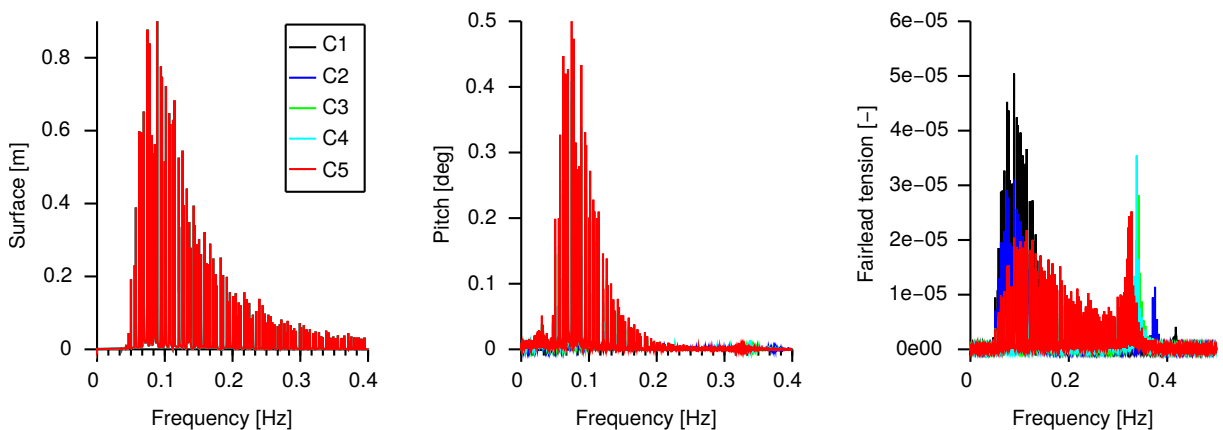

Figure 9: Surface elevation, pitch and normalised tendon tension in frequency domain

The fairlead tension peaks within $0.3 − 0.4Hz$ (Figure 9, right) suggest that pitch motion is the dominant frequency contributor to tendon excitation. As the tension response at pitch natural frequency configurations C3, C4 and C5 is significantly higher than C1

11

and C2, they also shows the widest τ/τ_0 range in Figure 6 at exceedance probability close to $P = 10^0$. On the other hand, C1 presents a higher response around $0.1Hz$, pointing at its high response to the most energetic interval of the sea spectrum. As bigger waves have lower frequencies and are more energy dense, surge becomes the dominant source of tendon excitation as the τ/τ_0 range in C1 becomes the widest.

VI – Conclusion

This paper discusses the effect of the incremental variation in tendon inclination on motion and tendon tension of the TLP DTU 10MW FOWT model. Time domain simulations were carried out using EDF Lab's fully coupled CAE tool DIEGO/CALHYPSO for the solution of the hydro-aero-servo-elastic problem. The numerical model was validated by comparison with basin experimental data [14]. Five design configurations were identified, which were subject to an irregular sea climate and, separately, to a steady wind of $15m/s$.

Under the 3-hour realisation of the irregular wave climate, changes in motion and tendon tension response were observed and compared for each tendon configuration. Surge motions were significantly reduced by increasing the inclination angle of the tendons, as it increased the horizontal component of the restoring forces. The peak surge displacement was reduced from $8m$ to a minimum of $6m$ as the tendons were inclined from $90deg$ (C1 - vertical lines) to $75.92deg$ (C5). Heave and pitch motions, on the contrary, were proportional to the tendon inclination angle. The tendon tension ratio τ/τ_0 had a peak range of $\pm50\%$ and $\pm33\%$ respectively for the upstream and downstream tendons in the vertical tendon configuration. This amplitude was reduced to a minimum range of $\pm20\%$ and $\pm15\%$ inclining the tendons at an angle of $79.18deg$ (C3). The mitigating effect of different FOWT designs on the negative aerodynamic damping effect was also observed, showing that inclined tendon configurations can significantly reduce the negative damping effects caused by the resonant coupling between the turbine and the pitch controller.

The initial results from this study indicate the significance of tendon inclination in FOWT designs to support development of the industry in achieving techno-economic viability. While the numerical model of the wind turbine and the floating platform were thoroughly validated against experimental results before conducting the simulations discussed in this paper, the authors recognise the uncertainties stemming from the numerical methods applied. These numerical methods are heavily relied upon in industry, with a number of assumptions being made in the attempt to find an acceptable trade-off between accuracy and computational efficiency. Dynamic inlet and wake effects were neglected in the aerodynamic model, which are expected to have an impact on the forces developed on the blades and tower. Future work will investigate the effect of higher order hydrodynamic loads and combined wind and wave climates, in order to observe the behaviour of the considered design solutions in realistic environmental conditions.

VII – Acknowledgements

References

[1] M. Abbas. La méthode des éléments finis isoparamétriques. Technical report, Code Aster, 2013. Report R3.01.00.

[2] A. Babarit and G. Delhommeau. Theoretical and numerical aspects of the open source bem solver nemoh. 11th European Wave and Tidal Energy Conference (EWTEC), 2015.

[3] E. E. Bachynski and T. Moan. Design considerations for tension leg platform wind turbines. *Marine Structures*, 29:89–114, 2012.

[4] C. Bak, F. Zahle, R. Bitsche, T. Kim, A. Yde, L. C. Henriksen, A. Natarajan, and M. Hansen. Description of the dtu 10 mw reference wind turbine. Technical report, DTU Wind Energy, 2013. Report-I-0092.

[5] M. Borg, M. Mirzaei, and H. Bredmose. Qualification of innovative floating substructures for 10mw wind turbines and water depths greater than 50m. Technical report, DTU Wind Energy, 2015. LIFES50+ Deliverable D1.2 Wind turbine models for the design, project 640741.

[6] T. Burton, N. Jenkins, D. Sharpe, and E. Bossanyi. *Wind Energy Handbook*. Wiley, 2 edition, 2011.

[7] W. Cummins. *The Impulse Response Function and Ship Motions*. Navy Department, David Taylor Model Basin, 1962.

[8] G. Delhommeau. *Seakeeping Codes AQUADYN and AQUAPLUS*. 1993. Proceedings of the 19th WEGEMT SCHOOL on Numerical Simulation of Hydrodynamics: Ships and Offshore Structures.

[9] M. Folley. *Numerical Modelling of Wave Energy Converters*. Academic Press, 2016.

[10] M. H. Hansen and L. C. Henriksen. Basic dtu wind energy controller. Technical report, DTU Wind Energy, 2013. E-0028.

[11] J. Jonkman. Influence of control on the pitch damping of a floating wind turbine. Conference paper NREL/CP-500-42589, 2008. Presented at the 2008 ASME Wind Energy Symposium in Reno, Nevada.

[12] J. M. Jonkman, S. Butterfield, W. Musial, and G. Scott. Definition of a 5 - mw reference wind turbine for offshore system development. Technical report, National Renewable Energy Laboratory (NREL), 2009. NREL/TP-500-38060.

[13] T. J. Larsen and T. D. Hanson. A method to avoid negative damped low frequent tower vibrations for a floating, pitch controlled wind turbine. *Journal of Physics: Conference Series*, 75(1), 2007.

[14] R. Laugesen and A. M. Hansen. Experimental study of the dynamic response of the dtu 10mw wind turbine on a tension leg platform. Master thesis, DTU Wind Energy, 2015.

[15] B. Molin. *Hydrodynamique des structures offshore*. Editions TECHNIP, 2002. Guides pratiques sur les ouvrages en mer.